

Boosting Point-BERT by Multi-choice Tokens

Kexue Fu^{12*}, Mingzhi Yuan^{12*}, Manning Wang^{12†}

¹Digital Medical Research Center, School of Basic Medical Science, Fudan University, Shanghai, China

²Shanghai Key Laboratory of Medical Image Computing and Computer Assisted Intervention, Shanghai, China
kxfu18@fudan.edu.cn, mzyuan20@fudan.edu.cn, mnwang@fudan.edu.cn

Abstract

Masked language modeling (MLM) has become one of the most successful self-supervised pre-training tasks. Inspired by its success, Point-BERT, as a pioneer work in point cloud, proposed masked point modeling (MPM) to pre-train point transformer on large scale unannotated dataset. Despite its great performance, we find the inherent difference between language and point cloud tends to cause ambiguous tokenization for point cloud. For point cloud, there doesn't exist a gold standard for point cloud tokenization. Point-BERT use a discrete Variational AutoEncoder (dVAE) as tokenizer, but it might generate different token ids for semantically-similar patches and generate the same token ids for semantically-dissimilar patches. To tackle above problem, we propose our McP-BERT, a pre-training framework with multi-choice tokens. Specifically, we ease the previous single-choice constraint on patch token ids in Point-BERT, and provide multi-choice token ids for each patch as supervision. Moreover, we utilize the high-level semantics learned by transformer to further refine our supervision signals. Extensive experiments on point cloud classification, few-shot classification and part segmentation tasks demonstrate the superiority of our method, e.g., the pre-trained transformer achieves 94.1% accuracy on ModelNet40, 84.28% accuracy on the hardest setting of ScanObjectNN and new state-of-the-art performance on few-shot learning. We also demonstrate that our method not only improves the performance of Point-BERT on all downstream tasks, but also incurs almost no extra computational overhead. The code will be released in <https://github.com/fukexue/McP-BERT>.

Introduction

Self-supervised pre-training (Grill et al. 2020; Chen and He 2021; He et al. 2021; Yang, Zhang, and Cui 2022; Ohri and Kumar 2021; Zhao and Dong 2020; Larsson, Maire, and Shakhnarovich 2017; He et al. 2020) is attracting growing attentions as it can transfer knowledge learned from large scale unlabeled dataset to boost the performance on downstream tasks. Most self-supervised pre-training methods are based on specific proxy tasks such as permutation prediction (Zhao and Dong 2020), image colorization (Larsson, Maire, and Shakhnarovich 2017), instance-level discrimination (Grill et al. 2020; Chen and He 2021; He et al. 2020).

Among them, the masked language modeling (MLM) task proposed in BERT (Devlin et al. 2018) is currently one of the most successful proxy tasks and has been migrated to many other domains (Bao, Dong, and Wei 2021; Li et al. 2022; Yu et al. 2022). Point-BERT (Yu et al. 2022), as a pioneer work in point cloud learning, proposed a variant of MLM called masked point modeling (MPM) to pre-train point cloud transformers. Specifically, it first divides a point cloud into several local point patches and assigns a token id to each patch to convert the point cloud into multiply discrete tokens. Then it masks a proportion of tokens and pre-trains the model by recovering the masked tokens based on the transformer encoding results of the corrupted point cloud. Since there is not well-defined vocabulary to generate token ids for local point cloud patches, Point-BERT utilizes a pre-trained discrete Variational AutoEncoder (dVAE) (Rolfe 2016) as the tokenizer. However, we find such discrete tokenization in MPM hinders the framework to achieve better performance due to the difference between point cloud and language.

Languages are naturally composed of discrete words, which are strictly bijective to the token ids. However, there is no such gold standard for point clouds discretization as for language, making it inevitable to introduce noise to MPM. Specifically, dVAE-based tokenization tends to cause the following two kinds of ambiguities. (1) Semantically-dissimilar patches have the same token ids. Due to the lack of well-defined vocabulary, MPM adopts a pre-trained dVAE as tokenizer to generate token ids for local patches. However, the tokenizer focuses on local patches' geometry but barely considers their semantics, resulting in some wrong token ids. For example, two patches shown in red in Figure 1 consist of similar geometric structure but have different semantics (landing gear and aero-engine). However, they are allocated with the same token ids (#3776) due to their similar geometric structure. (2) Semantically-similar patches have different token ids. As shown in Figure 1, semantically-similar patches of the aero-engine of the airplane are allocated with many different token ids (#599, #1274). It's reasonable for them to have the same token ids because of their similar semantics and geometry to each other. However, the tokenizer neglects their relations and allocates them with different token ids due to the interference of imperfect discretization and acquisition noise.

*These authors contributed equally.

†Corresponding Author.

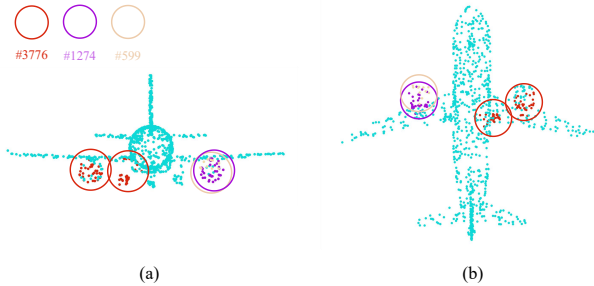


Figure 1: **Visualization of improper token ids.** To better visualize the improper tokenization, we provide two different views of the same point cloud. Different colors represent the different token ids, and the circles indicate the range of local patches. As shown in above two figures, semantically-dissimilar patches (landing gear and aero-engine, colored in red) have the same token ids (#3776), and semantically-similar adjacent patches (aero-engine, colored in purple and brown) have different token ids (#1274, #599).

Inspired by mc-BEiT (Li et al. 2022), we propose an improved BERT-style point cloud pre-training framework called McP-BERT with multi-choice tokens to tackle the above problems. Specifically, since semantically-similar patches might have different token ids, we ease the previous strict single-choice constraint on patch token ids. For each local patch, we utilize a probability distribution vector of token ids as supervision signal rather than previous single token id, which means each patch has Multi-Choice token ids. Moreover, we believe high-level perceptions produced by point cloud transformer can provide extra semantic supervision signals, which benefit our pre-training. Therefore, we refine the above supervision signals, i.e., the probability distribution vectors, using inter-patch semantic similarities, which come from our point cloud transformer. By considering high-level similarities, the ambiguities caused by local geometric similarity can be mitigated.

To verify the effectiveness of our framework, we pre-train a point cloud transformer on ShapeNet (Chang et al. 2015) and conduct extensive fine-tuning experiments on downstream tasks including point cloud classification, few-shot classification and part segmentation. Our framework not only improve the performance of previous Point-BERT on **all** downstream tasks, but also incurs almost no extra computational overhead during pre-training. Our McP-BERT achieves 94.1% accuracy on ModelNet40 (Wu et al. 2015) and 84.28% accuracy on the complicated setting of ScanObjectNN (Uy et al. 2019), outperforming a series of state-of-the-art methods. Our method also achieves new state-of-the-art on point cloud few-shot learning, indicating powerful generalization of our McP-BERT.

Related Works

Pre-training on large-scale data and then fine-tuning on target tasks has been proved to be an effective paradigm to boost the performance of model on downstream tasks (He, Girshick, and Dollár 2019). However, although many effi-

cient annotation tools (Wu et al. 2021; Girardeau-Montaut 2016) have been proposed, labeling a large-scale dataset is still costly especially for point cloud data. Therefore, self-supervised pre-training which pre-trains models without annotations has more potential. In the past few years, many self-supervised pre-training methods for point cloud learning had been proposed and the core of them is designing a proper proxy task. For example, Poursaeed et al. (Poursaeed et al. 2020) pre-trained networks by predicting point cloud’s rotation. Inspired by the success of a series of contrastive learning-based self-supervised method (Grill et al. 2020; Chen and He 2021; He et al. 2020), PointContrast (Xie et al. 2020) and STRL (Huang et al. 2021) implemented a contrastive learning paradigm to learn deep representations from depth scan. OcCo (Wang et al. 2021) pre-trained their encoder by reconstructing occluded point clouds. Recently, inspired great success of BERT (Devlin et al. 2018), Point-BERT (Yu et al. 2022) designed a proxy task called masked point modeling (MPM), following a mask-and-then-predict paradigm to pre-train point cloud transformer. Since there exist no vocabulary for officially break raw point clouds into small predefined chunks, Point-BERT incorporates a dVAE as tokenizer. It first divides a complete point cloud into several patches and then allocates token ids for patches based on dVAE’s latent features. However, we find that as we analyzed above, this improper tokenizer tends to produce ambiguous token ids for each patch. Therefore, we improve Point-BERT by introducing eased and refined token ids in this work.

Preliminaries

Similar to Point-BERT (Yu et al. 2022), we also adopt a Masked Point Modeling (MPM) paradigm as our proxy task to pre-train our model. Specifically, given a point cloud P , we first sample g center points $\{c_i\}_{i=1}^g$ using farthest point sampling (Lang, Manor, and Avidan 2020) and then select their k -nearest neighbor points to build g local patches $\{p_i\}_{i=1}^g$. The points in local patches are normalized by subtracting their center points to further mitigate their coordinate bias. Then a mini-PointNet (Qi et al. 2017a) is used to map the normalized patches to a sequence of patch embeddings $\{f_i\}_{i=1}^g$. The above process is shown in Figure 2(a). After that, a tokenizer will take embeddings as inputs and generate token ids $\{\hat{z}_i \in \mathbb{R}^{|V|}\}_{i=1}^g$ for patches, where $|V|$ denotes the length of the vocabulary V . As done in other BERT-style works, we randomly mask a proportion of tokens and then send corrupted patch embeddings into a backbone implemented by transformer encoder. The backbone will learn l_2 -normalized representations $\{h_i\}_{i=1}^g$ for both masked and unmasked tokens, as shown in Figure 2(b). Finally, we pre-train the backbone by predicting the masked tokens based on these representations. The objective of MPM can be formulated as follow:

$$\mathcal{L}_{MPM} = \mathbb{E}_{i \in M} \left[- \sum_{k=1}^{|V|} \hat{z}_{i,k} \log q(\hat{z}_{i,k} | h_i) \right] \quad (1)$$

where M denotes the set of masked patches, q denotes a MLP head to predict the token id \hat{z}_i of masked patch p_i

based on representation h_i . For Point-BERT, the token id \hat{z}_i is a one-hot vector, which is derived from latent feature z_i in dVAE:

$$\hat{z}_{i,k} = \begin{cases} 1 & \text{if } k = \arg \max_j z_{i,j} \\ 0 & \text{else} \end{cases} \quad (2)$$

where $z_i \in \mathbb{R}^{|V|}$ denotes latent feature in the dVAE’s encoder. However, as mentioned above and shown in Figure 1, this imperfect tokenizer will make some semantically-similar patches have different tokens and some semantically-dissimilar patches have the same tokens. To tackle these problems, we ease the token id \hat{z}_i to a soft vector satisfying $\sum_k \hat{z}_{i,k} = 1$, allowing one patch corresponds to multiply token ids. Moreover, we re-build \hat{z}_i based on the high-level semantic relationship for more accurate supervision. The details are presented in the next section.

Method

Our framework is shown in Figure 2, and we will introduce it in detail in this section. To verify the effectiveness of our proposed idea, we set Point-BERT as our baseline and modify it as little as possible.

Before pre-training, we train a dVAE (Rolfe 2016) as our tokenizer in the same way as in Point-BERT. During pre-training, transformer (Vaswani et al. 2017) encoder in our framework is trained on unlabeled data over MPM. For fine-tuning, the transformer encoder is first initialized with the pre-trained parameters, and all of the parameters are fine-tuned using labeled data from downstream tasks. We first briefly introduce the implements of the tokenizer and the transformer encoder. Then we provide details about our multi-choice strategy, which plays an important role in improving the tokenization.

Tokenizer

Our tokenizer is trained through dVAE-based point cloud reconstruction. As shown in Figure 2(d), the dVAE adopts an encoder-decoder architecture. The encoder is our tokenizer $Q_\phi(z^o | p)$, which consists of a DGCNN (Wang et al. 2019) and Gumbel-softmax (Jang, Gu, and Poole 2016). During training dVAE, DGCNN $Q_\phi(z | p)$ takes a sequence of patch embeddings as input and outputs latent features $\{z_i\}_{i=1}^g$. Then the latent features $\{z_i\}_{i=1}^g$ is discretized into one-hot vectors $\{z_i^o\}_{i=1}^g$ through a Gumbel-softmax. The decoder $P_\theta(p | z^o)$ consists of a DGCNN followed by a FoldingNet (Yang et al. 2018). DGCNN takes one-hot vectors $\{z_i^o\}_{i=1}^g$ as input and take full advantage of their neighborhood relationship in the feature space to enhance the representation of these discrete tokens. The following FoldingNet reconstructs the original point cloud according to DGCNN’s outputs. As with other VAE-style works (Kingma and Welling 2013), we achieve reconstruction objective by optimizing the evidence lower bound (ELBO) of the log-

likelihood $P_\theta(p | \tilde{p})$:

$$\begin{aligned} \sum_{(p_i, \tilde{p}_i) \in D} \log P_\theta(p_i | \tilde{p}_i) \geq \\ \sum_{(p_i, \tilde{p}_i) \in D} (\mathbb{E}_{z_i^o \sim Q_\phi(z^o | p_i)} [\log P_\theta(p_i | z_i^o)] \\ - KL[Q_\phi(z^o | p_i) \| P_\theta(z^o | \tilde{p}_i)]) \end{aligned} \quad (3)$$

where \tilde{p} denotes the reconstructed patches, D denotes the training corpus, $P_\theta(z^o | \tilde{p}_i)$ follows a uniform distribution. The former of ELBO represents the reconstruction loss and the latter represents the distribution loss. We follow (Yu et al. 2021) to calculate the reconstruction loss and follow (Ramesh et al. 2021) to optimize the distribution difference between one-hot vectors and prior. Our tokenizer has the same architecture as in Point-BERT (Yu et al. 2022) but outputs the latent features $\{z_i\}_{i=1}^g$ rather than the one-hot vectors $\{z_i^o\}_{i=1}^g$ during pre-training. More details about the architecture of tokenizer can refer to Point-BERT.

Transformer Encoder

We utilize a standard transformer (Vaswani et al. 2017) following Point-BERT’s settings as our backbone, as shown in Figure 2(b). During pre-training, we randomly mask a proportion of patch embeddings and fed them including masked and unmasked patch embeddings into the backbone. Then the backbone outputs the deep representations $\{h_{cls}\} \cup \{h_i\}_{i=1}^g$, where h_i represents the representations for both masked and unmasked patches and h_{cls} represents the representation for classification, as part of the input of classification head in the downstream task. The deep representations extracted by transformer consider the associations between patches and contain more semantic information, which is suitable for many downstream tasks and refining the supervision signals. We will go over how to use these representations to refine the supervision signals in the following section.

Multi-choice Tokenization

As mentioned above, there doesn’t exist a gold standard for point cloud tokenization. Therefore, it’s inevitable for tokenizer to produce improper supervision, including generating the same token ids for semantically-dissimilar patches and generating different token ids for semantically-similar patches. We observe that given a local patch, there may exist multiply suitable token ids as candidates as illustrated in Figure 1. Inspired by mc-BEiT (Li et al. 2022), we attempt to release the strict single-choice constraint on token ids. As shown in Figure 2(c), given a local patch p_i , we don’t use unique token id as supervision any more. Instead, we predict the probability distribution vector $\mathcal{P}(z_i) \in \mathbb{R}^{|V|}$ of the token ids. Specifically, the probability distribution vector $\mathcal{P}(z_i) \in \mathbb{R}^{|V|}$ is generated by a softmax operation:

$$\mathcal{P}(z_i)_k = \frac{\exp(z_{i,k}/\tau)}{\sum_{j=1}^{|V|} \exp(z_{i,j}/\tau)} \quad (4)$$

where $z_i \in \mathbb{R}^{|V|}$ denotes the latent feature in tokenizer, τ is a temperature coefficient, which controls the smoothness of

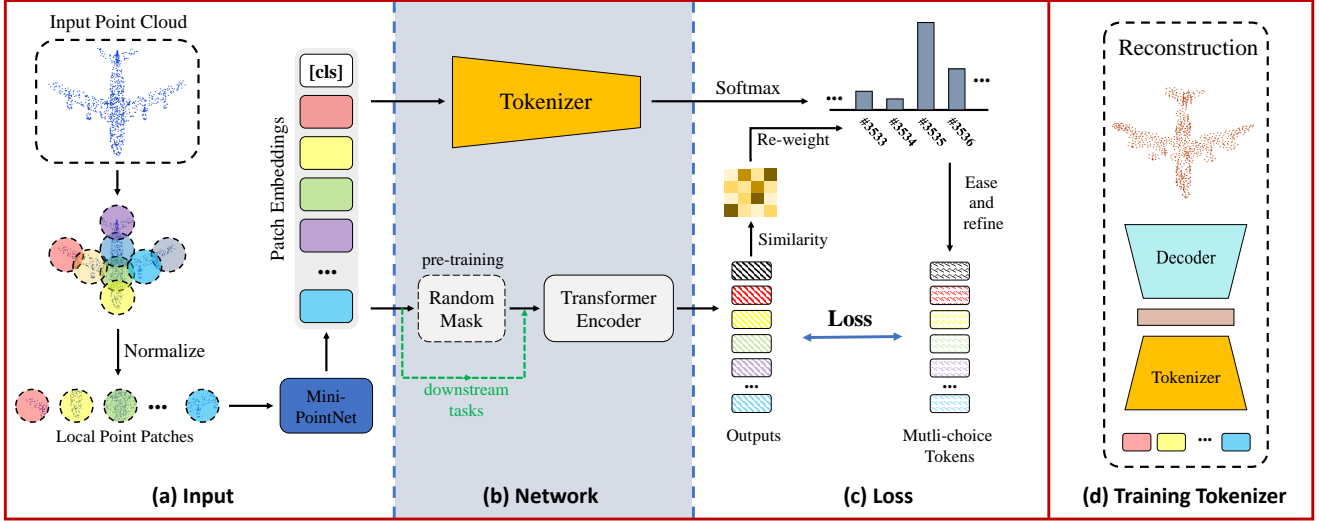


Figure 2: **Overview of our proposed method, McP-BERT.** We improve the Point-BERT by incorporating multi-choice tokens. We utilize a softmax layer to ease the hard token ids into soft probability distribution vectors of token ids and use the encoded features generated by transformer encoder to re-weight the soft probability distribution vectors. During pre-training, a proportion of tokens are randomly masked and fed into transformer encoder. The transformer encoder is optimized by predicting the masked eased and refined token signals in the form of a soft-label cross-entropy loss. Unlike pre-training, when applied to downstream tasks, we skip the random mask operation, which is represented by a dashed green line, and input all patch embeddings into the transformer encoder.

probability distribution. When τ is small, $\mathcal{P}(z_i)$ tends to be a one-hot vector. When τ is large, it is equivalent to incorporate more choices.

Moreover, to further tackle the ambiguity of token ids as shown in Figure 1, more high-level semantics should be incorporated. As analyzed in introduction, tokenizer focuses on encoding local geometry of local patches while ignoring the associations between patches, making semantically-dissimilar patches have the same token ids. To alleviate this problem, we use the representations learned by transformer to re-weight the probability distribution vectors as done in (Li et al. 2022). Specifically, as shown in Figure 2(c), we use the cosine similarity between patch features learned by transformer to re-weight the probability distribution matrix $\mathcal{P}(z) \in \mathbb{R}^{g \times |V|}$. The similarity matrix $W \in \mathbb{R}^{g \times g}$ is calculated as follows:

$$W_{i,k} = \frac{\exp \langle h_i, h_k \rangle}{\sum_{j=1}^g \exp \langle h_i, h_j \rangle} \quad (5)$$

where h_i denotes the l_2 -normalized representations learned by transformer, $\langle \cdot, \cdot \rangle$ denotes the inner product between two vectors. The refined probability distribution matrix $W\mathcal{P}(z)$ considers the inter-patch associations, making semantically-similar patches have more similar probability distributions and semantically-dissimilar patches have more discriminable probability distributions.

The final targets \hat{z} for prediction is a weighted sum of the eased probability distribution matrix $\mathcal{P}(z)$ and the refined probability distribution matrix $W\mathcal{P}(z)$:

$$\hat{z} = \omega \mathcal{P}(z) + (1 - \omega) W\mathcal{P}(z) \quad (6)$$

where ω is a coefficient balancing the low-level semantics from tokenizer and high-level semantics from inter-patch similarity. Slightly different from mc-BEiT (Li et al. 2022), we adopt a warm-up strategy, i.e. gradually decreasing ω rather than a constant one. Specifically, at the beginning of pre-training, we set $\omega = 1$ due to inadequate training of transformer. After 30 epochs, transformer can well encode both the local geometry of local patches and dependencies between patches. Then the coefficient ω begins to decrease in a cosine schedule to boost pre-training. We set the lower bound of ω as 0.8. Our experiments also show this gradually decreasing paradigm plays an essential role in the pre-training. When we set ω to a constant at the beginning, the transformer is easy to collapse due to the noisy semantics from initial transformer.

Experiment

In this section, we first introduce the setup of pre-training. Then we conduct experiments on downstream tasks including point cloud classification, few-shot learning and part segmentation. We also present various ablations to analyze the effectiveness of our method and provide visualizations of our learned representations. Furthermore, we also compare the computational overhead of our McP-BERT with Point-BERT. **Our code will be publicly available.**

Pre-training

For all experiments, we use ShapeNet (Chang et al. 2015) as the pre-training dataset, which originally contains over 50,000 CAD models from 55 common object categories. We

Table 1: **Comparisons of the classification on ModelNet40** (Wu et al. 2015). * represents training from scratch.

Method	Acc (%)
PointNet (Qi et al. 2017a)	89.2
PointNet++ (Qi et al. 2017b)	90.5
PointCNN (Li et al. 2018)	92.2
DGCNN (Wang et al. 2019)	92.2
DensePoint (Liu et al. 2019a)	92.8
KPConv (Thomas et al. 2019)	92.9
PTC (Guo et al. 2021)	93.2
PointTransformer (Zhao et al. 2021)	93.7
GLR (Rao, Lu, and Zhou 2020)	92.9
SRTL (Huang et al. 2021)	93.1
Transformer*	91.4
OcCo (Wang et al. 2021)	92.2
Point-BERT (Yu et al. 2022)	93.8
Ours	94.1

randomly sample 1024 points from each CAD model and divide them into 64 local patches. Each patch contains 32 points. For the BERT-style pre-training, we randomly mask 25 ~ 45% patches for MPM in a block masking manner (Yu et al. 2022). For more details of implementation, please refer to the supplementary materials.

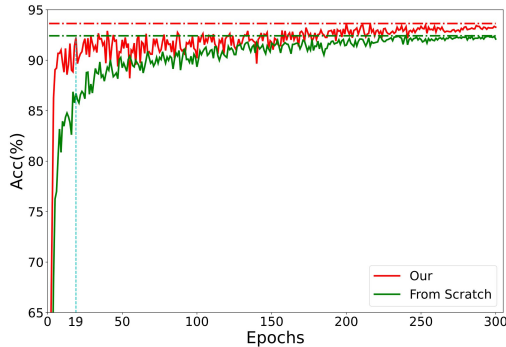


Figure 3: **Convergence curve.** We compare the performance of transformers training from scratch (green) and pre-training with our method (red) in terms of validation accuracy (%) on ModelNet40. The red dotted line denotes the best performance of our method while the green dotted line denotes the best performance of the baseline. Our method reaches baseline’s best performance in only 19 epochs.

Point Cloud Classification

We perform our classification experiments on both the synthetic dataset ModelNet40 (Wu et al. 2015) and real-world dataset ScanObjectNN (Uy et al. 2019).

Experiment on Synthetic Dataset: ModelNet40 (Wu et al. 2015) is the most popular 3D dataset for point cloud classification, which contains 12311 CAD models from 40 object categories. We randomly sample 8k points from each

Table 2: **Comparisons of the classification on ScanObjectNN** (Uy et al. 2019). We report the accuracy (%) of three different settings (OBJ-BG, OBJ-ONLY, PB-T50-RS). * represents training from scratch.

Method	OBJ-BG	OBJ-ONLY	PB-T50-RS
PointNet	73.3	79.2	68.0
SpiderCNN	77.1	79.5	73.7
PointNet++	82.3	84.3	77.9
PointCNN	86.1	85.5	78.5
DGCNN	82.8	86.2	78.1
BGA-DGCNN	-	-	79.7
BGA-PN++	-	-	80.2
Transformer*	79.86	80.55	77.24
OcCo	84.85	85.54	78.79
Point-BERT	87.43	88.12	83.07
Ours	88.98	90.02	84.28

CAD model for training and test. We follow previous setting (Qi et al. 2017a; Wu et al. 2021) to split the dataset into 9843/2468 for training and test.

Competitors: We compare our method with supervised methods, i.e., PointNet (Qi et al. 2017a), PointNet++ (Qi et al. 2017b), PointCNN (Li et al. 2018), DGCNN (Wang et al. 2019), DensePoint (Liu et al. 2019a), KPConv (Thomas et al. 2019), PCT (Guo et al. 2021), PointTransformer (Zhao et al. 2021) and recently published self-supervised pre-training methods (Yu et al. 2022; Huang et al. 2021; Wang et al. 2021; Rao, Lu, and Zhou 2020). Moreover, to illustrate the effectiveness of pre-training, we also set a baseline model, which use the same backbone model as ours but trained from scratch.

Results: We adopt the classification accuracy as the evaluation metric and the experiment results are listed in Table 1. As observed from the results, our method obtain 94.1% accuracy on ModelNet40, outperforming the competitive methods and achieving new state-of-the-art performance. We also provide a convergence curve in Figure 3. We can see our method improves the baseline by 2.7% and converges to a high performance faster. Our method also outperforms Point-BERT by 0.3% with negligible extra computational overhead, which indicates the effectiveness of our multi-choices strategy.

Experiment on Real-world Dataset: To test our method’s generalization to real scenes, we also conduct an experiment on a real-world dataset. ScanObjectNN (Uy et al. 2019) is a dataset modified from scene mesh datasets SceneNN (Hua et al. 2016) and ScanNet (Dai et al. 2017). It contains 2902 point clouds from 15 categories. We follow previous works (Yu et al. 2022; Uy et al. 2019) to carry out experiments on three variants: OBJ-BG, OBJ-ONLY and PB-T50-RS, which denote the version with background, the version without background and the version with random perturbations, respectively. More details can be found in (Uy et al. 2019).

Competitors: We compare our method with supervised methods, i.e., PointNet (Qi et al. 2017a), SpiderCNN (Xu et al. 2018), PointNet++ (Qi et al. 2017b), PointCNN (Li

Table 3: **Few-shot classification results on ModelNet40** (Wu et al. 2015). We list the average accuracy (%) and the standard deviation over 10 independent experiments. * represents training from scratch.

	5-way		10-way	
	10-shot	20-shot	10-shot	20-shot
3D GAN	55.8±3.4	65.8±3.1	40.3±2.1	48.4±1.8
FoldingNet	33.4±4.1	35.8±5.8	18.6±1.8	15.4±2.2
L-GAN	41.6±5.3	46.2±6.2	32.9±2.9	25.5±3.2
3D-Caps	42.3±5.5	53.0±5.9	38.0±4.5	27.2±4.7
PointNet	52.0±3.8	57.8±4.9	46.6±4.3	35.2±4.8
PointNet++	38.5±4.4	42.4±4.5	23.1±2.2	18.8±1.7
PointCNN	65.4±2.8	68.6±2.2	46.6±1.5	50.0±2.3
RSCNN	65.4±8.9	68.6±7.0	46.6±4.8	50.0±7.2
DGCNN	31.6±2.8	40.8±4.6	19.9±2.1	16.9±1.5
Transformer*	87.8±5.2	93.3±4.3	84.6±5.5	89.4±6.3
OcCo	94.0±3.6	95.9±2.3	89.4±5.1	92.4±4.6
Point-BERT	94.6±3.1	96.3±2.7	91.0±5.4	92.7±5.1
Ours	97.1±1.8	98.3±1.2	92.4±4.3	94.9±3.7

et al. 2018), DGCNN (Wang et al. 2019), models equipped with background-aware (Uy et al. 2019) (BGA) module and some state-of-the-art self-supervised pre-training methods (Yu et al. 2022; Wang et al. 2021). In this experiment, we also set a baseline as we do on ModelNet40.

Results: The classification accuracy on ScanObjectNN is shown in Table 2. As observed from the results, all the methods perform worse on real-world dataset than on synthetic dataset ModelNet40, which is caused by less data for fine-tuning and the interference of noise, background, occlusion, etc. However, our method still achieves best performances on all three variants. It’s worth noting that our method significantly improves the baseline by 9.12%, 9.47%, and 7.04% on the three variants, which strongly confirms the generalization of our method. The above results also indicate that pre-training can transfer useful knowledge to downstream task and plays important roles in downstream task especially when downstream task is challenging.

Few-shot Learning

Few-shot learning aims to tackle new tasks containing limited labeled training examples using prior knowledge.

Dataset: Here we conduct experiments on ModelNet40 (Wu et al. 2015) to evaluate our method. All our experiments follow K-way, m-shot setting (Sharma and Kaul 2020). Specifically, we randomly select K classes and sample m+20 samples for each class. The model is trained on K*m samples (support set), and evaluated on K*20 samples (query set). We compare our method with other competitors under “5 way, 10 shot”, “5 way, 20 shot”, “10 way, 10 shot”, “10 way, 20 shot” settings and report the mean and standard deviation over 10 runs.

Competitors: Our competitors can be roughly divided into three categories: (1) unsupervised methods; (2) supervised methods; (3) self-supervised pre-training methods. For the unsupervised methods (Yang et al. 2018; Wu et al. 2016; Achlioptas et al. 2018; Zhao et al. 2019), we train a lin-

ear SVM based on their extracted unsupervised representations. For supervised methods (Qi et al. 2017a,b; Wang et al. 2019; Li et al. 2018; Liu et al. 2019b) including our baseline, we train the model from scratch. For self-supervised pre-training methods (Yu et al. 2022; Wang et al. 2021) including our McP-BERT, we fine-tune the model with pre-trained weight as initializations.

Results: The results are shown in Table 3. We can see that when the labeled training data is insufficient, our method can still perform well. Our method has the highest average accuracy under four different settings. It’s noticeable that compared with other methods, our method commonly has a smaller standard deviation, which indicates our method is more stable. Our method also significantly improves the baseline by 9.3%, 5.2%, 7.8%, and 5.5%, which demonstrates the strong generalization ability of our method.

Point Cloud Part Segmentation

Point cloud part segmentation is a challenging task aimed at predicting point-wise label for point cloud. Here, we evaluate our method on the widely used ShapeNetPart (Yi et al. 2016) dataset.

Dataset: ShapeNetPart contains 16881 CAD models from 16 object categories, annotated with 50 parts. We follow the setting in (Qi et al. 2017a) to randomly sample 2048 points from each CAD model for training and test. We also double the number of local patches to 128 in the pre-training for part segmentation.

Competitors: We compare our method with some widely used methods (Qi et al. 2017a,b; Wang et al. 2019) and recently published self-supervised pre-training methods (Yu et al. 2022; Wang et al. 2021). We also adopt a standard transformer trained from scratch as our baseline.

Results: We evaluate all the methods on two types of $mIoU$, i.e. $mIoU_C$ and $mIoU_I$. The former denotes the mean IoU across all part categories and the later denotes the mean IoU across all instances. As shown in Table 4, our method achieves the best performance on both metrics. Our method also boosts baseline’s performance while OcCo fails to do so. In addition, please refer to the supplementary material for the IOU of each category and the visualization of segmentation.

Ablation Study

In this section, we conduct extensive experiments on ModelNet40 (Wu et al. 2015) to study the effect of hyperparameters.

The temperature coefficient τ : The hyperparameter τ controls the smoothness of supervision signals. When τ is small, we will get a sharp probability distribution of token ids. And conversely, when τ is large, the probability distribution tends to be a uniform distribution. To study the effect of τ , we conduct an ablation study on τ and the result is shown on Table 5. We also add a single-choice version i.e., the same as in Point-BERT as competitor, which equals to $\tau \rightarrow 0$. Observed from the result, we find our multi-choice strategy performs best when temperature coefficient is set to 0.005 empirically and improves previous BERT-style pre-training.

Table 4: **Part segmentation results on the ShapeNetPart** (Yi et al. 2016). We report the mean IoU across all part categories $mIoU_C$ (%) and the mean IoU across all instances $mIoU_I$ (%), as well as the IoU (%) for each categories. * represents training from scratch.

	PointNet	PointNet++	DGCNN	Transformer*	OcCo	Point-BERT	Ours
$mIoU_C$	80.4	81.9	82.3	83.4	83.4	84.1	84.4
$mIoU_I$	83.7	85.1	85.2	85.1	85.1	85.6	86.1

Table 5: **Ablation study on the temperature coefficient** τ . The ablation is conducted on point cloud classification downstream task on ModelNet40 (Wu et al. 2015).

	Single-choice (Point-BERT)	Multi-choice			
		0.005	0.05	0.5	5
Acc (%)	93.8	94.1	93.6	93.5	93.6

Table 6: **Ablation study on the weight coefficient** ω . The ablation is conducted on point cloud classification downstream task on ModelNet40 (Wu et al. 2015).

	0	0.2	0.4	0.6	0.8	1.0
Acc (%)	93.5	93.4	93.6	93.6	94.1	93.8
	w/o warm up		Point-BERT			
Acc (%)	collapse		93.8			

The weight coefficient ω : The hyperparameter ω balances the low-level semantics from tokenizer and high-level semantics from transformer encoder. We conduct an ablation study on ω and the result is shown on Table 6. In this ablation study, we not only compare our McP-BERT under different ω settings, but also compare with a baseline, i.e., Point-BERT and a version without warm up strategy for ω . In the version without warm up, we set $\omega = 0.8$ at the beginning of the pre-training rather than progressively decreasing ω after pre-training several epochs. Observed from the result, the version without warm up collapses during the pre-training, because the transformer is not well-trained enough to provides accurate semantics. Moreover, pre-training seems to perform better as the weight coefficient ω goes larger. But when $\omega = 1.0$, the supervision signals don't incorporate high-level semantics, making the pre-training has the same performance as the baseline. As can be seen from the above, both the warm up strategy and the high-level semantics generated from transformer play important roles. See supplementary materials for more ablation studies.

Visualization

To further understand the effectiveness of our method, we visualize the learned features via t-SNE (Van der Maaten and Hinton 2008). Figure 4(a) shows our learned features before fine-tuning. As observed from it, features are well separated even trained without annotations, which are suitable for model initialization. Figure 4(b) and (c) provide visualization of features fine-tuned on ModelNet40 (Wu et al. 2015) and ScanObjectNN (Uy et al. 2019). As can be seen, features form multiply clusters that are far away from each other, indicating the effectiveness of our method.

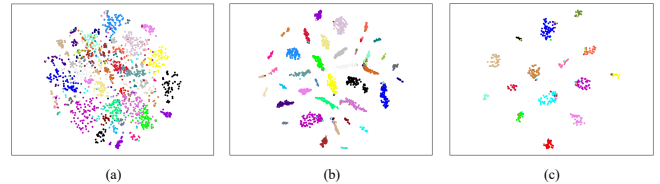


Figure 4: **Visualization of feature distributions.** We utilize t-SNE (Van der Maaten and Hinton 2008) to visualize the features learned by our McP-BERT. Features from different categories are visualized in different colors. (a) Features after pre-training; (b) Features fine-tuned on ModelNet40; (c) Features fine-tuned on ScanObjectNN.

Table 7: **Comparisons of the time overhead of pre-training.**

	Point-BERT	Ours
Running time (s/epoch)	143.48	144.94

Computational Overhead

To demonstrate that our method improves the performance while introducing almost no extra computational overhead, we compare to the computational overhead of Point-BERT (Yu et al. 2022) on the same device. The pre-training is implemented on an Intel Xeon Platinum 8260 CPU and two RTX3090 GPU. We select the time overhead of each pre-training epoch as our evaluation metric. As shown in Table 7, our method only incurs 1% extra time consuming, which is almost negligible.

Conclusion

In this paper, we propose McP-BERT, a BERT-style pre-training method for point cloud pre-training, which tackles the problem of improper tokenizer in previous work. We release the previous strict single-choice constraint on token ids and utilize the probability distribution vector of token ids as supervision signals to avoid semantically-similar patches corresponding to different token ids. In addition, we use the high-level semantics generated by transformer to re-weight the probability distribution vector to further avoid semantically-dissimilar patches corresponding to the same token ids. Extensive experiments on different datasets and downstream tasks are conducted to evaluate the performance of our McP-BERT. The results show that our McP-BERT not only improves the performance of previous work on all downstream tasks with almost no extra computational overhead, but also achieve new state-of-the-art on point cloud classification and point cloud few-shot learning. The exper-

iments also reveal that our pre-training method successfully transfer knowledge learned from unlabeled data to downstream tasks, which has great potential in point cloud learning.

References

- Achlioptas, P.; Diamanti, O.; Mitliagkas, I.; and Guibas, L. 2018. Learning representations and generative models for 3d point clouds. In *International conference on machine learning*, 40–49. PMLR.
- Bao, H.; Dong, L.; and Wei, F. 2021. Beit: Bert pre-training of image transformers. *arXiv preprint arXiv:2106.08254*.
- Chang, A. X.; Funkhouser, T.; Guibas, L.; Hanrahan, P.; Huang, Q.; Li, Z.; Savarese, S.; Savva, M.; Song, S.; Su, H.; et al. 2015. Shapenet: An information-rich 3d model repository. *arXiv preprint arXiv:1512.03012*.
- Chen, X.; and He, K. 2021. Exploring simple siamese representation learning. In *Proceedings of the IEEE/CVF Conference on Computer Vision and Pattern Recognition*, 15750–15758.
- Dai, A.; Chang, A. X.; Savva, M.; Halber, M.; Funkhouser, T.; and Nießner, M. 2017. Scannet: Richly-annotated 3d reconstructions of indoor scenes. In *Proceedings of the IEEE conference on computer vision and pattern recognition*, 5828–5839.
- Devlin, J.; Chang, M.-W.; Lee, K.; and Toutanova, K. 2018. Bert: Pre-training of deep bidirectional transformers for language understanding. *arXiv preprint arXiv:1810.04805*.
- Girardeau-Montaut, D. 2016. CloudCompare. *France: EDF R&D Telecom ParisTech*.
- Grill, J.-B.; Strub, F.; Altché, F.; Tallec, C.; Richemond, P.; Buchatskaya, E.; Doersch, C.; Avila Pires, B.; Guo, Z.; Gheshlaghi Azar, M.; et al. 2020. Bootstrap your own latent—a new approach to self-supervised learning. *Advances in Neural Information Processing Systems*, 33: 21271–21284.
- Guo, M.-H.; Cai, J.-X.; Liu, Z.-N.; Mu, T.-J.; Martin, R. R.; and Hu, S.-M. 2021. Pct: Point cloud transformer. *Computational Visual Media*, 7(2): 187–199.
- He, K.; Chen, X.; Xie, S.; Li, Y.; Dollár, P.; and Girshick, R. 2021. Masked autoencoders are scalable vision learners. *arXiv preprint arXiv:2111.06377*.
- He, K.; Fan, H.; Wu, Y.; Xie, S.; and Girshick, R. 2020. Momentum contrast for unsupervised visual representation learning. In *Proceedings of the IEEE/CVF conference on computer vision and pattern recognition*, 9729–9738.
- He, K.; Girshick, R.; and Dollár, P. 2019. Rethinking imagenet pre-training. In *Proceedings of the IEEE/CVF International Conference on Computer Vision*, 4918–4927.
- Hua, B.-S.; Pham, Q.-H.; Nguyen, D. T.; Tran, M.-K.; Yu, L.-F.; and Yeung, S.-K. 2016. Scenenn: A scene meshes dataset with annotations. In *2016 Fourth International Conference on 3D Vision (3DV)*, 92–101. IEEE.
- Huang, S.; Xie, Y.; Zhu, S.-C.; and Zhu, Y. 2021. Spatio-temporal self-supervised representation learning for 3d point clouds. In *Proceedings of the IEEE/CVF International Conference on Computer Vision*, 6535–6545.
- Jang, E.; Gu, S.; and Poole, B. 2016. Categorical reparameterization with gumbel-softmax. *arXiv preprint arXiv:1611.01144*.
- Kingma, D. P.; and Welling, M. 2013. Auto-encoding variational bayes. *arXiv preprint arXiv:1312.6114*.
- Lang, I.; Manor, A.; and Avidan, S. 2020. Samplenet: Differentiable point cloud sampling. In *Proceedings of the IEEE/CVF Conference on Computer Vision and Pattern Recognition*, 7578–7588.
- Larsson, G.; Maire, M.; and Shakhnarovich, G. 2017. Colorization as a proxy task for visual understanding. In *Proceedings of the IEEE conference on computer vision and pattern recognition*, 6874–6883.
- Li, X.; Ge, Y.; Yi, K.; Hu, Z.; Shan, Y.; and Duan, L.-Y. 2022. mc-BEiT: Multi-choice Discretization for Image BERT Pre-training. *arXiv preprint arXiv:2203.15371*.
- Li, Y.; Bu, R.; Sun, M.; Wu, W.; Di, X.; and Chen, B. 2018. Pointcnn: Convolution on x-transformed points. *Advances in neural information processing systems*, 31.
- Liu, Y.; Fan, B.; Meng, G.; Lu, J.; Xiang, S.; and Pan, C. 2019a. Densepoint: Learning densely contextual representation for efficient point cloud processing. In *Proceedings of the IEEE/CVF International Conference on Computer Vision*, 5239–5248.
- Liu, Y.; Fan, B.; Xiang, S.; and Pan, C. 2019b. Relation-shape convolutional neural network for point cloud analysis. In *Proceedings of the IEEE/CVF Conference on Computer Vision and Pattern Recognition*, 8895–8904.
- Ohri, K.; and Kumar, M. 2021. Review on self-supervised image recognition using deep neural networks. *Knowledge-Based Systems*, 224: 107090.
- Poursaeed, O.; Jiang, T.; Qiao, H.; Xu, N.; and Kim, V. G. 2020. Self-supervised learning of point clouds via orientation estimation. In *2020 International Conference on 3D Vision (3DV)*, 1018–1028. IEEE.
- Qi, C. R.; Su, H.; Mo, K.; and Guibas, L. J. 2017a. Pointnet: Deep learning on point sets for 3d classification and segmentation. In *Proceedings of the IEEE conference on computer vision and pattern recognition*, 652–660.
- Qi, C. R.; Yi, L.; Su, H.; and Guibas, L. J. 2017b. Pointnet++: Deep hierarchical feature learning on point sets in a metric space. *Advances in neural information processing systems*, 30.
- Ramesh, A.; Pavlov, M.; Goh, G.; Gray, S.; Voss, C.; Radford, A.; Chen, M.; and Sutskever, I. 2021. Zero-shot text-to-image generation. In *International Conference on Machine Learning*, 8821–8831. PMLR.
- Rao, Y.; Lu, J.; and Zhou, J. 2020. Global-local bidirectional reasoning for unsupervised representation learning of 3d point clouds. In *Proceedings of the IEEE/CVF Conference on Computer Vision and Pattern Recognition*, 5376–5385.
- Rolfe, J. T. 2016. Discrete variational autoencoders. *arXiv preprint arXiv:1609.02200*.

- Sharma, C.; and Kaul, M. 2020. Self-supervised few-shot learning on point clouds. *Advances in Neural Information Processing Systems*, 33: 7212–7221.
- Thomas, H.; Qi, C. R.; Deschard, J.-E.; Marcotegui, B.; Goulette, F.; and Guibas, L. J. 2019. Kpconv: Flexible and deformable convolution for point clouds. In *Proceedings of the IEEE/CVF international conference on computer vision*, 6411–6420.
- Uy, M. A.; Pham, Q.-H.; Hua, B.-S.; Nguyen, T.; and Yeung, S.-K. 2019. Revisiting point cloud classification: A new benchmark dataset and classification model on real-world data. In *Proceedings of the IEEE/CVF international conference on computer vision*, 1588–1597.
- Van der Maaten, L.; and Hinton, G. 2008. Visualizing data using t-SNE. *Journal of machine learning research*, 9(11).
- Vaswani, A.; Shazeer, N.; Parmar, N.; Uszkoreit, J.; Jones, L.; Gomez, A. N.; Kaiser, Ł.; and Polosukhin, I. 2017. Attention is all you need. *Advances in neural information processing systems*, 30.
- Wang, H.; Liu, Q.; Yue, X.; Lasenby, J.; and Kusner, M. J. 2021. Unsupervised point cloud pre-training via occlusion completion. In *Proceedings of the IEEE/CVF International Conference on Computer Vision*, 9782–9792.
- Wang, Y.; Sun, Y.; Liu, Z.; Sarma, S. E.; Bronstein, M. M.; and Solomon, J. M. 2019. Dynamic graph cnn for learning on point clouds. *Acm Transactions On Graphics (tog)*, 38(5): 1–12.
- Wu, J.; Zhang, C.; Xue, T.; Freeman, B.; and Tenenbaum, J. 2016. Learning a probabilistic latent space of object shapes via 3d generative-adversarial modeling. *Advances in neural information processing systems*, 29.
- Wu, T.-H.; Liu, Y.-C.; Huang, Y.-K.; Lee, H.-Y.; Su, H.-T.; Huang, P.-C.; and Hsu, W. H. 2021. ReDAL: Region-based and Diversity-aware Active Learning for Point Cloud Semantic Segmentation. In *Proceedings of the IEEE/CVF International Conference on Computer Vision*, 15510–15519.
- Wu, Z.; Song, S.; Khosla, A.; Yu, F.; Zhang, L.; Tang, X.; and Xiao, J. 2015. 3d shapenets: A deep representation for volumetric shapes. In *Proceedings of the IEEE conference on computer vision and pattern recognition*, 1912–1920.
- Xie, S.; Gu, J.; Guo, D.; Qi, C. R.; Guibas, L.; and Litany, O. 2020. Pointcontrast: Unsupervised pre-training for 3d point cloud understanding. In *European conference on computer vision*, 574–591. Springer.
- Xu, Y.; Fan, T.; Xu, M.; Zeng, L.; and Qiao, Y. 2018. Spidercnn: Deep learning on point sets with parameterized convolutional filters. In *Proceedings of the European Conference on Computer Vision (ECCV)*, 87–102.
- Yang, X.; Zhang, Z.; and Cui, R. 2022. TimeCLR: A self-supervised contrastive learning framework for univariate time series representation. *Knowledge-Based Systems*, 245: 108606.
- Yang, Y.; Feng, C.; Shen, Y.; and Tian, D. 2018. Foldingnet: Point cloud auto-encoder via deep grid deformation. In *Proceedings of the IEEE conference on computer vision and pattern recognition*, 206–215.
- Yi, L.; Kim, V. G.; Ceylan, D.; Shen, I.-C.; Yan, M.; Su, H.; Lu, C.; Huang, Q.; Sheffer, A.; and Guibas, L. 2016. A scalable active framework for region annotation in 3d shape collections. *ACM Transactions on Graphics (ToG)*, 35(6): 1–12.
- Yu, X.; Rao, Y.; Wang, Z.; Liu, Z.; Lu, J.; and Zhou, J. 2021. Pointr: Diverse point cloud completion with geometry-aware transformers. In *Proceedings of the IEEE/CVF International Conference on Computer Vision*, 12498–12507.
- Yu, X.; Tang, L.; Rao, Y.; Huang, T.; Zhou, J.; and Lu, J. 2022. Point-BERT: Pre-training 3d point cloud transformers with masked point modeling. In *Proceedings of the IEEE/CVF Conference on Computer Vision and Pattern Recognition*, 19313–19322.
- Zhao, H.; Jiang, L.; Jia, J.; Torr, P. H.; and Koltun, V. 2021. Point transformer. In *Proceedings of the IEEE/CVF International Conference on Computer Vision*, 16259–16268.
- Zhao, Q.; and Dong, J. 2020. Self-supervised representation learning by predicting visual permutations. *Knowledge-Based Systems*, 210: 106534.
- Zhao, Y.; Birdal, T.; Deng, H.; and Tombari, F. 2019. 3D point capsule networks. In *Proceedings of the IEEE/CVF Conference on Computer Vision and Pattern Recognition*, 1009–1018.